Talanta 125 (2014) 29–35

Contents lists available at ScienceDirect

Talanta

journal homepage: www.elsevier.com/locate/talanta

Studies of gold nanorod-iron oxide nanohybrids for immunoassay based on SPR biosensor

Hua Zhang [a], Ying Sun [a], Shang Gao [a], Hanqi Zhang [a], Jia Zhang [a], Yu Bai [b], Daqian Song [a,*]

[a] College of Chemistry, Jilin University, Qianjin Street 2699, Changchun 130012, PR China
[b] Beijing National Laboratory for Molecular Sciences, College of Chemistry and Molecular Engineering, Peking University, Beijing 100871, PR China

ARTICLE INFO

Article history:
Received 25 November 2013
Received in revised form
17 February 2014
Accepted 18 February 2014
Available online 27 February 2014

Keywords:
Surface plasmon resonance (SPR)
GNR-Fe_3O_4 nanohybrids
Biosensor
Mouse IgG

ABSTRACT

A wavelength modulation surface plasmon resonance (SPR) biosensor based on gold nanorods-Fe_3O_4 (GNR-Fe_3O_4) nanohybrids was developed for the determination of mouse IgG. The premade negatively charged Fe_3O_4 nanoparticles were coated on the surface of positively charged GNRs through electrostatic interaction. The synthetic method was simple, quick and easy operation. The aldehyde group functionalized GNR-Fe_3O_4 nanohybrids possess unique magnetic property, exceptional optical property and good biocompatibility, which can be used as immobilization matrix for biomolecules. The magnetic nanohybrids can be easily immobilized on the surface of SPR biosensor chip with a magnetic pillar, which simplifies the experimental procedure. The effects of GNR-Fe_3O_4 nanohybrids on the sensitivity of SPR biosensor were also studied. The SPR biosensor based on GNR-Fe_3O_4 nanohybrids shows a good response to mouse IgG in the concentration range of 0.15–40.00 μg mL^{-1}, while the biosensor based on MPA and Fe_3O_4 nanoparticles show a good response to mouse IgG in the concentration range of 2.50–40.00 μg mL^{-1} and 1.25–40.00 μg mL^{-1}, respectively. As a result, when GNR-Fe_3O_4 nanohybrids were used in SPR biosensor, the sensitivity for the determination of mouse IgG is significantly enhanced.

1. Introduction

The synthetic procedures of nanoparticles in different shapes and sizes have been evolved in the past few years. There are plenty of methods for the nanoparticles preparation including chemical vapor deposition [1], molecular beam epitaxy [2], and colloid chemistry approach [3]. Especially, the wet chemical synthesis is of great advantages, for it provides a tight control of particle size and shape, as well as easy operation and low cost [4]. Depending on the nature of materials, nanoparticles show particular properties such as surface plasmon resonance (SPR) for noble metals [5], magnetic response for iron or cobalt [6], and luminescence for semiconductors [7]. It is still a major challenge to obtain novel nanohybrids containing more than one property, which will broaden new technological applications. The hybrid nanostructures can be divided into two types, core-shell structures and heterodimers. Core-shell nanohybrids consist of a nanocrystalline core and another nanomaterial shell. As for heterodimers, two or more domains are connected through a small interfacial area. With different synthetic methods, many systems of nanohybrids have been obtained such as metallic–metallic [8,9], metallic-semiconductor [10,11], magnetic–metallic [12,13] and semiconductor–magnetic [14]. In each case, the photoluminescence properties, optical properties and magnetic properties can be improved as compared to those of single-component nanoparticles.

Metallic nanoparticles, especially noble metal nanoparticles have unique optoelectronic properties, which provide a promising application for chemical sensing [15–17]. Noble metal nanoparticles are highly sensitive to the refractive index (RI) of their surface bound materials and surrounding environment [18]. The increase in RI of the surrounding environment results in a red shift of surface plasmon wavelength of noble metal nanoparticles. Gold nanoparticles exhibit well-defined optical properties depending on their geometric shape and size. The difference between gold nanorods (GNRs) and spherical gold nanoparticles is that GNRs show two absorption bands: one associated with the transverse mode (~520 nm), and the other with the longitudinal mode (> 600 nm, usually the end region of visible or near infrared region) [19]. Importantly, the longitudinal plasmon wavelength is more sensitive to the changes in the dielectric properties of the surrounding, and the sensitivity increases with the aspect ratio of the nanorods [20,21]. Magnetic nanoparticles have been of scientific and technological interest due to their potential applications in biosensors [22], drug delivery [23], bioseparation [24], and molecular interaction in live cells [25]. Owing to the super paramagnetic property and high ratio of surface area to volume, magnetic nanoparticles can be used as immobilization matrix and are easy to be separated from liquid phase by the magnetic field. Therefore, to take full advantages of GNRs and magnetic

* Corresponding author. Tel.: +86 431 85168399; fax: +86 431 85112355.
E-mail address: songdq@jlu.edu.cn (D. Song).

http://dx.doi.org/10.1016/j.talanta.2014.02.036
0039-9140

nanoparticles, the as-prepared positively charged GNRs were coated with negatively charged Fe_3O_4 nanoparticles through electrostatic interaction to obtain the GNR-Fe_3O_4 nanohybrids, which were further used in SPR biosensor.

SPR biosensor is a powerful tool to investigate the interaction between biomolecules, especially antibody-antigen complexes because of its characteristics of simplicity, label-free, high selectivity and real-time monitoring [26,27]. As a quantitative tool, SPR biosensor can be used to determine reaction kinetic and affinity constants for molecular interaction, as well as the active concentration of biomolecules in solution. A variety of SPR biosensors have been developed and applied for the detection of specific analytes in the area of biotechnology, medical diagnosis, environmental protection and food safety [28]. In SPR measurements, effective immobilization of biomolecules on the sensor surface plays a crucial role in enhancing the sensitivity of SPR biosensor. Different kinds of sensing membranes, such as colloidal Au [29], TiO_2 film [30], Au/Ag alloy nanocomposites [31] and graphene oxide [32] were applied in SPR biosensor to immobilize biomolecules.

In this paper, Fe_3O_4 nanoparticles coated GNRs were prepared and used in SPR biosensor for the determination of mouse IgG. The GNR-Fe_3O_4 nanohybrids have both the advantages of GNRs and Fe_3O_4 nanoparticles. The magnetic nanohybrids can be assembled on the sensor surface using a magnetic pillar without any chemical covalent link, which greatly simplify the immunoassay procedures. And glutaraldehyde was used as the bridge to bind the antibody and the nanohybrids. Thus the bindings of antibody to antigen lead to changes in the RI on the sensor surface, which can be detected by the SPR biosensor.

2. Experimental

2.1. Materials

Mouse IgG, goat anti-mouse IgG, and human IgG were purchased from Beijing Biosynthesis Biotechnology Company. Bovine serum albumin (BSA) was purchased from Ding Guo Biotechnology Company (Beijing,China). Hydrogen tetrachloroauratehydrate ($HAuCl_4 \cdot 3H_2O$) was purchased from Acrosl. Ferric chloride hexahydrate ($FeCl_3 \cdot 6H_2O$), ferrous chloride tetrahydrate ($FeCl_2 \cdot 4H_2O$), sodium hydroxide, trisodium citrate, 3-aminopropyltrimethoxysilane (APTMS), glutaraldehyde, silver nitrate, ethanol, cetyltrimethylammonium bromide (CTAB), ascorbic acid and all other chemicals were of analytical reagent grade. All the solutions were prepared with ultra pure water, and all the glassware was cleaned with aqua regia before the experiments.

Mouse IgG, goat anti-mouse IgG, and human IgG were stored at −20 °C. Sodium phosphate buffered saline (PBS, 0.01 mol L^{-1}, pH 7.4) was used as running buffer.

2.2. Equipment

In this paper, the wavelength modulation SPR biosensor installed in our laboratory was used (Fig. S1). Kretschmann configuration was applied to achieve the resonant condition by attenuated total reflection (ATR) in a prism. It is based on fixing the incident angle and monitoring the resonant wavelength at which the intensity of the reflected light is lowest. A glass slide with 50 nm Au film was put on base of a prism (K9 glass) using a suitable index matching oil (cedar oil). The light emitted from the halogen tungsten lamp is polarized to produce transverse magnetic (TM) polarized light. Two lenses are employed to make the light parallel. The parallel polychromatic light beam passes through the optical prism and excites surface plasmon at the interface between the Au film and the analytes. The output light from the prism is guided into the optical fiber and then enters the spectrophotometer (Ocean Optics, Inc., USA). A 2048 element linear array charge-coupled device (CCD) was used as the detector. The incident angle is fixed to make sure that SPR occurs. A magnetic pillar was set under the optical prism and the Au film was in the magnetic field of 750 G that was measured with Tesla meter. When the analyte is injected into the flow cell, it produces a change of the refractive index near the biosensor surface, which is observed as the shift of resonance wavelength. All SPR measurements were carried out at room temperature.

2.3. Assay procedure

2.3.1. Synthesis of citrate-capped Fe_3O_4 nanoparticles

The Fe_3O_4 nanoparticles were prepared by chemical coprecipitation methods [33]. Briefly, 2.6 g of $FeCl_3 \cdot 6H_2O$ and 1.0 g of $FeCl_2 \cdot 4H_2O$ were dissolved in 100 mL of deionized water. Under nitrogen gas protection, 12 mL of 25% $NH_3 \cdot H_2O$ was added drop by drop with vigorous mechanical stirring. After 30 min, the obtained Fe_3O_4 nanoparticles were isolated from the solution with a permanent magnet and washed with deionized water four times. The nanoparticles were dispersed in 100 mL of deionized water. To prepare citrate-capped Fe_3O_4 nanoparticles, 1 mL of the above Fe_3O_4 nanoparticles solution was added into 20 mL of 10% trisodium citrate solution and then sonicated for 20 min. Trisodium citrate is a kind of hydrophilic surfactant. The citrate ion can be adsorbed on the surface of Fe_3O_4 nanoparticles and form a relatively close-packed layer. There are three carboxyl groups in every citrate ion, and the repulsive forces between the electric charges of the radical ions make Fe_3O_4 nanoparticles more dispersed in water. The magnetic nanoparticles were isolated from the mixture with a permanent magnet and redispersed into 20 mL of deionized water.

2.3.2. Synthesis of aldehyde group functionalized GNR-Fe_3O_4 nanohybrids

GNRs were first synthesized through a seed-mediated method with CTAB used as a stabilizer [34]. To 10 mL of GNRs solution, 1 mL of the premade citrate-capped Fe_3O_4 nanoparticles solution was added. The mixture was vortexed for a few seconds and sat undisturbed for 45 min. The resulting solution was centrifuged at 7000 rpm for 5 min to remove the unbound Fe_3O_4 nanoparticles and the obtained nanohybrids were redispersed in 10 mL of deionized water.

The resultant GNR-Fe_3O_4 nanohybrids solution was mixed with APTMS in ethanol solution (v/v, 4/100) under stirring for 4 h at room temperature. The magnetic nanohybrids were isolated from the solution using a permanent magnet and washed with ethanol and deionized water successively. Then the amino group functionalized nanohybrids were immersed in 2% glutaraldehyde aqueous solution under stirring for 1 h at room temperature to get the aldehyde group functionalized GNR-Fe_3O_4 nanohybrids. The modified nanohybrids were isolated from the solution using a permanent magnet and redispersed in deionized water.

In contrast, the single Fe_3O_4 nanoparticles were also functionalized with aldehyde group by the same way as mentioned above. The prepared GNR-Fe_3O_4 nanohybrids and Fe_3O_4 nanoparticles were both stored at 4 °C when they were not used.

2.3.3. Preparation of SPR biosensor based on the modified GNR-Fe_3O_4 nanohybrids

The glass slide with Au film was fixed under the flow cell equipped with a magnetic pillar under the prism. Deionized water was first injected into the flow cell. Then the aldehyde group functionalized GNR-Fe_3O_4 nanohybrids solution was injected into the flow cell. Thus the nanohybrids can be immobilized on the Au

film through magnetic action, which produced a change of refractive index that could be observed as a red shift of the SPR resonant wavelength. After the modified GNR-Fe_3O_4 nanohybrids were immobilized, PBS was injected into the flow cell as the baseline solution. And a solution of goat anti-mouse IgG was introduced into the flow cell to covalently attach to aldehyde-activated surface. Ethanolamine hydrochloride solution (pH 8.0, 1 mol L^{-1}) was used to block the non-specific binding sites on the biosensor surface. 10 min later, PBS was injected into the flow cell to wash off non-covalently bound antibody and stabilize the baseline. A schematic illustration of the experimental procedure is shown in Fig. 1.

Meanwhile, the aldehyde group functionalized Fe_3O_4 nanoparticles were also used to immobilize goat anti-mouse IgG. The procedure was the same as that stated above. For comparison, the traditional biosensor based on MPA self-assemble monolayer (SAM) was also constructed. PBS was first injected into the flow cell as the baseline solution and 10 mmol L^{-1} MPA was injected to covalent attach onto Au film through Au-S bonding. After 2 h, the carboxyl group of MPA was activated with NHS under the catalysis of EDC for 20 min. Then goat anti-mouse IgG solution was injected and can be bound with MPA through the covalent attachment between the amine group and the carboxyl group. The following processes were the same as those mentioned above.

2.3.4. Immunoassay

At room temperature, mouse IgG at different concentrations diluted with PBS was separately injected into the flow cell. Due to the immunoreaction between mouse IgG in the solution and goat anti-mouse IgG immobilized on the biosensor surface, a shift of resonant wavelength can be measured by SPR biosensor. After 40 min, PBS buffer was injected into the flow cell and another sample solution was injected.

To evaluate the selectivity of the method stated above, human IgG and BSA were determined by the same procedure as used to determine mouse IgG.

2.3.5. Regeneration

After a series of antibody-antigen immunoassays were performed, the sensing membrane of the SPR biosensor was regenerated. The magnetic pillar was taken away from the bottom of the prism and water was injected into the flow cell to wash away the GNR-Fe_3O_4 nanohybrids coupled with goat anti-mouse IgG. After 30 min, the conjugates could be removed from the Au film and the resonant wavelength returned to the initial wavelength.

3. Results and discussions

3.1. Characterization of GNR-Fe_3O_4 nanohybrids

The morphologies of the magnetic nanohybrids were characterized by transmission electronic microscopy (TEM). Fig. 2 provides the TEM images of the prepared GNRs and GNR-Fe_3O_4 nanohybrids. As shown in Fig. 2a, the average particle size of GNRs is about 46 × 15 nm. When Fe_3O_4 nanoparticles were introduced, it can be clearly seen from Fig. 2b that the surface of GNRs was coated by Fe_3O_4 nanoparticles and the average size of Fe_3O_4 nanoparticles is about 10 nm. However, there is some aggregation of nanoparticles, because Fe_3O_4 nanoparticles were synthesized in water phase and pure magnetic nanoparticles are easy to aggregate due to the high surface energy. Fig. 3 shows the UV-vis absorption spectra of Fe_3O_4 nanoparticles, GNRs and GNR-Fe_3O_4 nanohybrids. The absorbance of Fe_3O_4 nanoparticles decreases with the increase of the wavelength and no obvious absorption peak is observed. As for GNRs, there are two absorption peaks, the transverse resonance peak located at 518 nm and the longitudinal resonance peak at 682 nm. After coated with Fe_3O_4 nanoparticles, a change in the slope and broadening of resonance peaks of GNRs can be observed, which is due to the swamping of the plasmon peak by contributions from Fe_3O_4 nanoparticles. And both the transverse and longitudinal resonance peaks show a red shift, indicating the surface modification of GNRs. Meanwhile, X-ray photoelectron spectroscopy (XPS) was used to identify the composition of prepared GNR-Fe_3O_4 nanohybrids. The binding energy of C (1 s) at 284.8 eV was used as an internal reference. It can be seen from Fig. 4a that the Au 4f spectrum is resolved into two spin-orbit components. The Au $4f_{7/2}$ and $4f_{5/2}$ peaks occur at the binding energies of 83.1 eV and 86.8 eV, respectively, which are consistent with metallic gold [35]. Fig. 4b shows the Fe 2p spectrum with the binding energies of 710.6 eV and 725.3

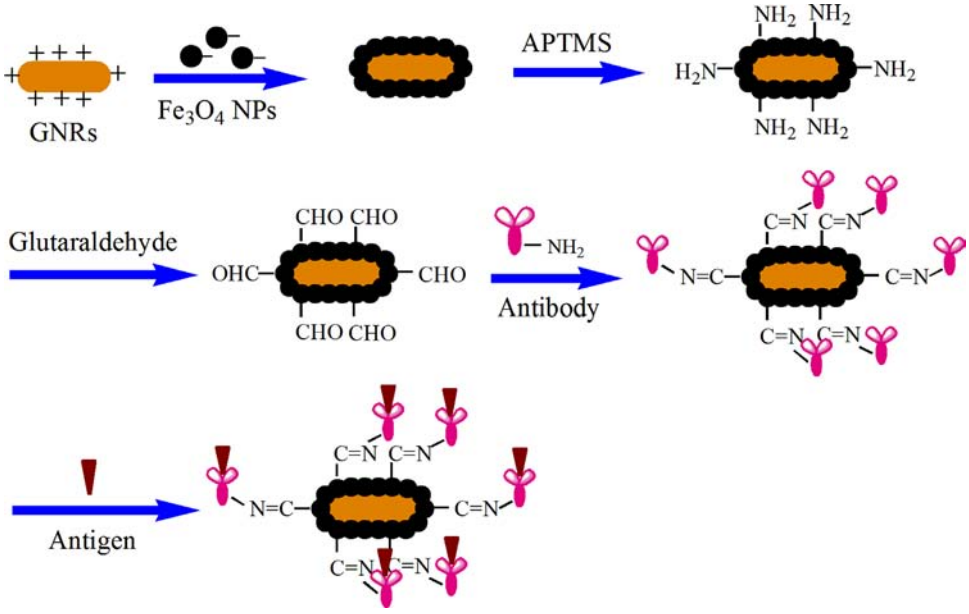

Fig. 1. Schematic diagram of the experimental procedure.

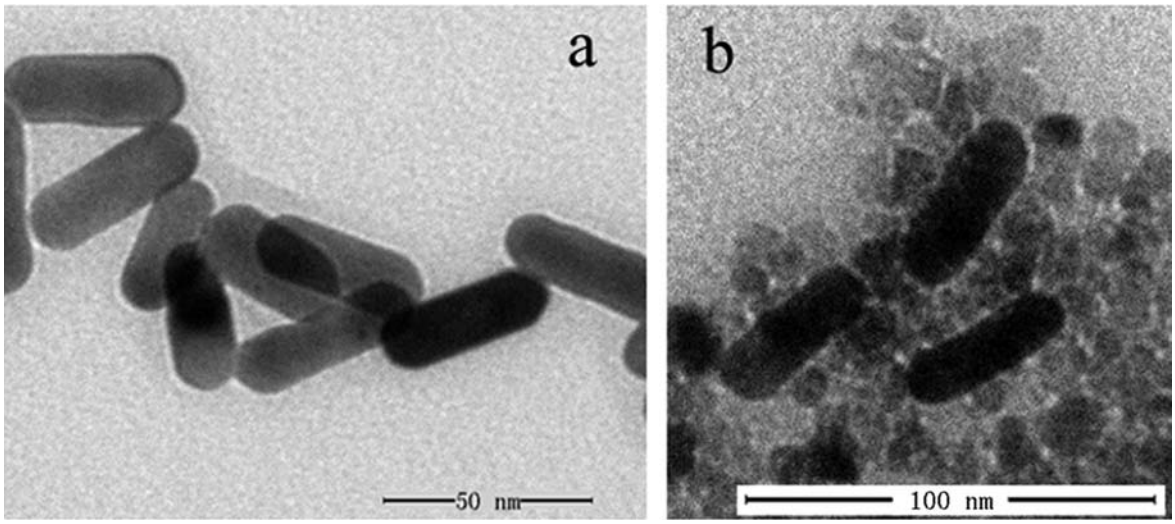

Fig. 2. TEM images of GNRs (a) and GNR-Fe_3O_4 nanohybrids (b).

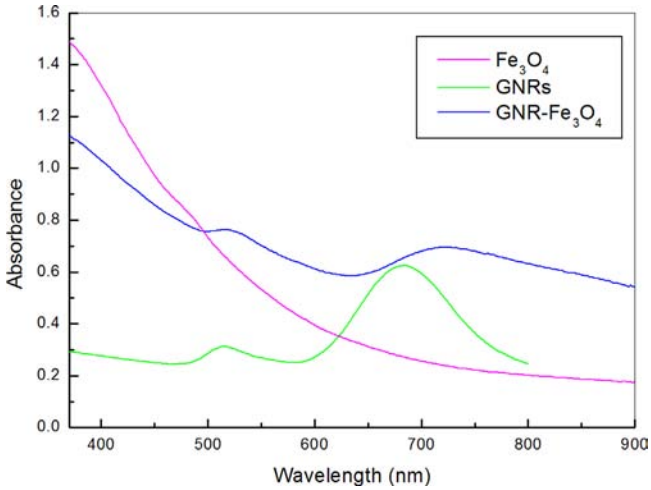

Fig. 3. UV–vis absorption spectra of Fe_3O_4 nanoparticles, GNRs and GNR-Fe_3O_4 nanohybrids.

eV, which correspond to Fe $2p_{3/2}$ and Fe $2p_{1/2}$, respectively, and the broad peak at 717.8 eV corresponds to Fe^{3+} [36]. The results indicated that GNR-Fe_3O_4 nanohybrids were synthesized successfully.

3.2. Preparation of SPR biosensor based on GNR-Fe_3O_4 nanohybrids

Traditionally, molecular self-assembly was applied to activate the SPR sensor surface for the immobilization of antibody, which requires many different reagents as the link. However, in this work the magnetic nanohybrids can be easily immobilized on the bare Au film with the magnetic pillar under the prism. When the GNR-Fe_3O_4 nanohybrids solution was injected into the flow cell, the shift of the resonant wavelength was monitored in real time. The maximum shift of the resonant wavelength reached about 8 nm, which was due to the increase of the thickness of the SPR sensing membrane and the changes of the refractive index arising from the interparticle interaction in the GNR-Fe_3O_4 nanohybrids. The red shift demonstrated that the GNR-Fe_3O_4 nanohybrids were immobilized on the Au film. Compared with the traditional SPR biosensor, the SPR biosensor based on GNR-Fe_3O_4 nanohybrids is easy to be constructed owing to the magnetic property of Fe_3O_4, which greatly simplifies the modification of sensing membrane to immobilize the antibody. On the other hand, the nanohybrids have large surface area for the immobilization of antibody and GNRs could be used to amplify the signal of SPR biosensor.

3.3. Immobilization of goat anti-mouse IgG

To select the optimal concentration of goat anti-mouse IgG coupled with GNR-Fe_3O_4 nanohybrids, goat anti-mouse IgG at different concentrations was separately injected into the flow cell after the aldehyde group functionalized GNR-Fe_3O_4 nanohybrids were immobilized on the Au film. The amine group of the antibody can be bound with the terminal aldehyde group of the nanohybrids through Schiff alkali reaction. Fig. 5 exhibits the kinetic adsorption curves of immobilizing goat anti-mouse IgG at different concentrations. The terminal aldehyde group shows a strong response to antibody and the antibody can be immobilized on the biosensor surface steadily. It can be seen that the shifts of resonant wavelength ($\Delta\lambda$) increased evidently at first and all reached about 85% of total shifts within 1 h. Finally, the resonant wavelength tends to be stable when the time is longer than 120 min, which indicates the immobilization of goat anti-mouse IgG on the biosensor surface was completed. Due to the increase of the concentration of goat anti-mouse IgG, more and more antibodies were immobilized on the biosensor surface, resulting in the resonant wavelength moving to longer wavelength. Once the antibody immobilized on the surface reached saturation, the resonant wavelength no longer changed and kept stable in a certain value. As shown in Fig. 5, when the concentrations of goat anti-mouse IgG are 50, 75, and 100 μg mL^{-1}, the shifts of resonant wavelength are 5.95, 8.16 and 8.38 nm, respectively. Therefore, 75 μg mL^{-1} was chosen as the optimal concentration of goat anti-mouse IgG for the detection of mouse IgG.

As a contrast, the biosensors based on single Fe_3O_4 nanoparticles and MPA were also experimented to study the effects of GNR-Fe_3O_4 nanocomposites on the performance improvement of SPR biosensor. Fig. 6 shows the kinetic adsorption curves of goat anti-mouse IgG at the concentration of 75 μg mL^{-1} on the surface of different biosensors. It can be seen that the maximum resonant wavelength shifts are 5.53, 6.40, and 8.16 nm for the biosensors based on MPA, Fe_3O_4 nanoparticles and GNR-Fe_3O_4 nanohybrids, respectively. The results indicated that the aldehyde group functionalized GNR-Fe_3O_4 nanohybrids is a good support for the immobilization of antibody. Due to the large surface area of Fe_3O_4 nanoparticles and

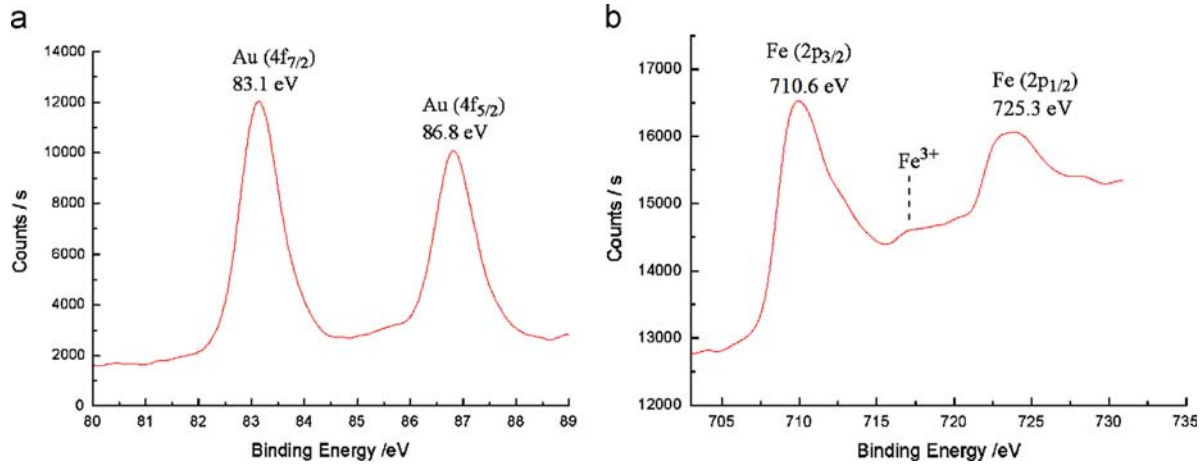

Fig. 4. X-ray photoelectron spectra of Au (a) and Fe (b).

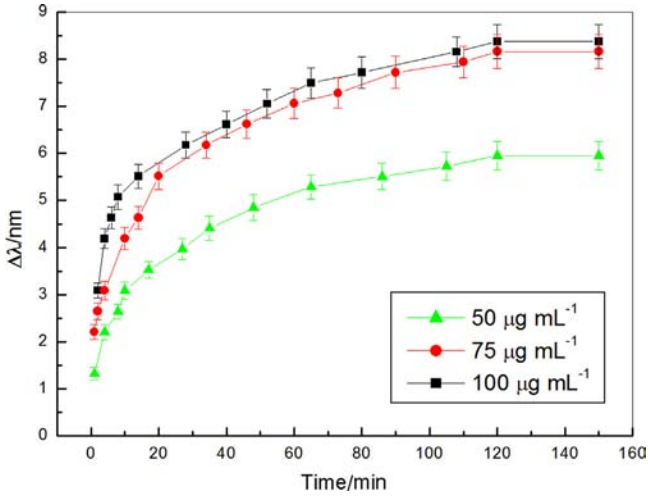

Fig. 5. Kinetic adsorption curves of immobilizing goat anti-mouse IgG on SPR biosensor based on GNR-Fe_3O_4 nanohybrids.

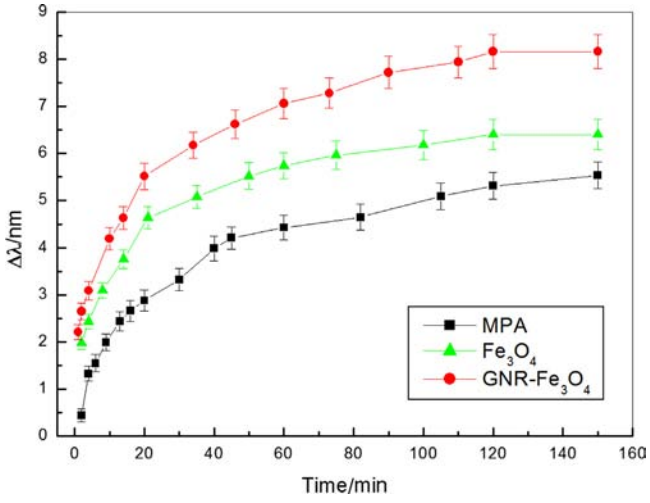

Fig. 6. Kinetic adsorption curves of immobilizing goat anti-mouse IgG at the concentration of 75 μg mL^{-1} on SPR biosensors based on MPA, Fe_3O_4 nanoparticles and GNR-Fe_3O_4 nanohybrids.

optoelectronic property of GNRs, when the biosensor based on GNR-Fe_3O_4 nanohybrids was used, the maximum resonant wavelength shift shows a modest increase.

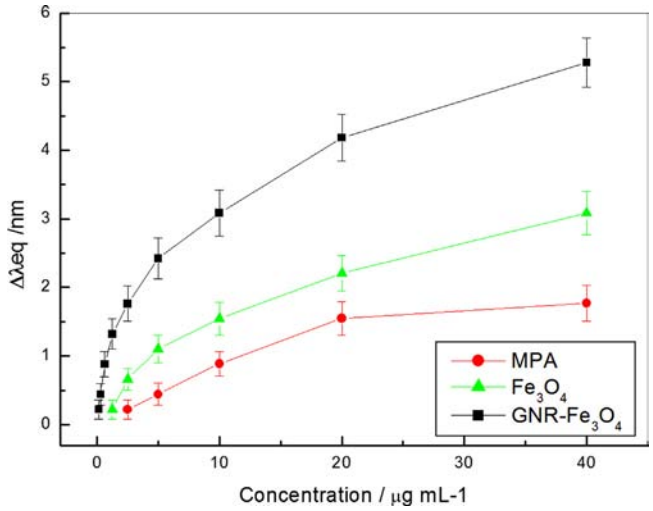

Fig. 7. The relationship between the concentrations of mouse IgG and the shifts of resonant wavelength obtained with the biosensor based on MPA, Fe_3O_4 nanoparticles and GNR-Fe_3O_4 nanohybrids.

3.4. Determination of mouse IgG

After goat anti-mouse IgG was immobilized on the sensor surface, mouse IgG at different concentrations was separately injected into the flow cell. The immunoreaction between the antibody and antigen occurring on the sensor surface leads to changes in the RI that is performed as the shift of resonant wavelength. With the increase of the concentration of mouse IgG, the shift of resonant wavelength gradually increased, which can be measured in real time by SPR biosensor. Fig. 7 displays the relationship between the shifts of resonant wavelength and the concentrations of mouse IgG. For the SPR biosensor based on MPA, it exhibits a response to mouse IgG in the concentration range of 2.50–40.00 μg mL^{-1}. The minimum shift of resonant wavelength is 0.22 nm at 2.50 μg mL^{-1} and the maximum shift of resonant wavelength is 1.77 nm at 40.00 μg mL^{-1}. The SPR biosensor based on Fe_3O_4 nanoparticles exhibits a response to mouse IgG in the concentration range of 1.25–40.00 μg mL^{-1}. The minimum shift of resonant wavelength is 0.22 nm at 1.25 μg mL^{-1} and the maximum shift of resonant wavelength is 3.08 nm at 40.00 μg mL^{-1}. The SPR biosensor based on GNR-Fe_3O_4 nanohybrids exhibits a good response to mouse IgG in the concentration range of 0.15–40.00 μg mL^{-1}. The minimum shift of resonant wavelength is 0.22 nm at 0.15 μg mL^{-1} and the maximum shift of resonant

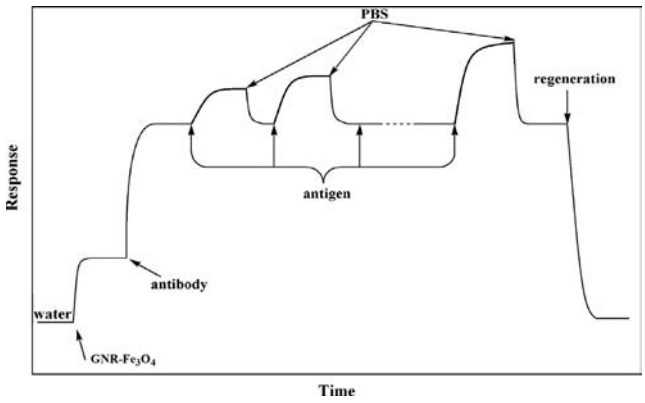

Fig. 8. The competitive SPR response curve for the detection of antigen.

wavelength is 5.28 nm at 40.00 μg mL^{-1}. The experimental results demonstrate the advantages of using GNR-Fe_3O_4 nanohybrids as SPR substrate for the immunoassay analysis. Under identical conditions, the lowest concentration determined by the biosensor based on GNR-Fe_3O_4 nanohybrids is lower than those determined by the biosensors based on MPA and Fe_3O_4 nanoparticles, and the signal of SPR biosensor was also enhanced.

When GNR-Fe_3O_4 nanohybrids were used, a significant increase in sensitivity is obtained in SPR biosensor. The detection of biomolecules interaction on SPR sensor chip is achieved by measuring the changes of RI and the film thickness on the sensor surface. The surface plasmon of GNRs might be resonantly excited through energy transfer in the near field and produce a strong local electromagnetic field. The interaction between the localized SPR of GNRs and the propagating plasmon in the Au film led to great changes of SPR reflectivity via strong optical coupling, which is mostly responsible for the sensitivity enhancement of SPR biosensor. Meanwhile, the use of GNR-Fe_3O_4 nanohybrids made the thickness of sensing membrane increase and the resonant wavelength move to longer wavelength. According to theoretical analysis, the shift of resonant wavelength towards a long wavelength could increase the sensitivity of the wavelength modulation SPR biosensor [37]. As stated above, the application of GNR-Fe_3O_4 nanohybrids in SPR biosensor has enhanced the sensitivity significantly.

The evaluation of the specificity was performed by detecting human IgG and BSA. After the goat anti-mouse IgG was immobilized on the biosensor surface, human IgG and BSA at the concentration of 10 μg mL^{-1} were separately injected into the flow cell for 40 min. There were no observable shifts of the resonant wavelength, which indicated the selective binding with mouse IgG (Fig. S2).

3.5. Regeneration of SPR biosensor

After the magnetic pillar was taken away from under the prism and water was injected into the flow cell, the GNR-Fe_3O_4 nanohybrids coupled with goat anti-mouse IgG could be dissociated from Au film. The SPR response curve of the whole cycle is shown in Fig. 8, including the immobilization of GNR-Fe_3O_4 nanohybrids and antibody, the binding of antigen at different concentrations and the regeneration of the biosensor. When the Au film was regenerated, new nanohybrids can be introduced into the flow cell for the next measurement.

4. Conclusions

The aldehyde group functionalized GNR-Fe_3O_4 nanohybrids were successfully synthesized and used in the wavelength modulation SPR biosensor for mouse IgG detection. The structures of GNR-Fe_3O_4 nanohybrids were separately characterized by TEM, UV–vis absorption spectroscopy and XPS. The GNR-Fe_3O_4 nanohybrids could be easily immobilized on the sensor surface by a magnetic pillar and have been demonstrated to be an ideal support for the sensitive detection of biomolecules. The SPR biosensor based on GNR-Fe_3O_4 nanohybrids displays a good response to mouse IgG in the concentration range of 0.15–40.00 μg mL^{-1}. The lowest concentration of mouse IgG that can be detected with the proposed biosensor is lower than those detected with the biosensor based on Fe_3O_4 nanoparticles and the biosensor based on MPA. Therefore, the GNR-Fe_3O_4 nanohybrids are beneficial to improve the performance of SPR biosensor.

Acknowledgments

This work was supported by the National Natural Science Foundation of China (Nos. 20727003, 21075049, 21105037), Program for New Century Excellent Talents in University (No. NECT-10-0443), Science and Technology Developing Foundation of Jilin Province (Nos. 20100356, 20110162), and Special-funded Program on National Key Scientific Instruments and Equipment Development (Nos. 2012YQ090194).

Appendix A. Supporting information

Supplementary data associated with this article can be found in the online version at http://dx.doi.org/10.1016/j.talanta.2014.02.036.

References

[1] S.J. Park, Y.Y. Choi, J.G. Kim, D.J. Choi, J. Cryst. Growth 361 (2012) 189.
[2] S. Garrido, V.M. Kaganer, K.K. Sabelfeld, T. Gotschke, J. Grandal, E. Calleja, L. Geelhaar, O. Brandt, Nano Lett. 13 (2013) 3274.
[3] L.M. Marzán, J. Mater. Chem. 16 (2006) 3891.
[4] T.K. Sau, C.J. Murphy, J. Am. Chem. Soc. 126 (2004) 8648.
[5] M. Mitsushio, K. Miyashita, M. Higo, Sens. Actuators A 125 (2006) 296.
[6] E.V. Shevchenko, D.V. Talapin, H. Schnablegger, A. Kornowski, O. Festin, P. Svedlindh, M. Haase, H. Weller, J. Am. Chem. Soc. 125 (2003) 9090.
[7] H.B. Zeng, W.P. Cai, P.S. Liu, X.X. Xu, H.J. Zhou, C. Klingshirn, H. Kalt, ACS Nano 2 (2008) 1661.
[8] S. Pyne, P. Sarkar, S. Basu, G.P. Sahoo, D.K. Bhui, H. Bar, A. Misra, J. Nanopart. Res. 13 (2011) 1759.
[9] L. Shang, L.H. Jin, S.J. Guo, J.F. Zhai, S.J. Dong, Langmuir 26 (2010) 6713.
[10] G.Y. Shan, M.Y. Zhong, S. Wang, Y.J. Li, Y.C. Liu, J. Colloid Interface Sci. 326 (2008) 392.
[11] L. Carbone, S. Kudera, C. Giannini, G. Ciccarella, R. Cingolani, P.D. Cozzoli, L. Manna, J. Mater. Chem. 16 (2006) 3952.
[12] H. Yu, M. Chen, P.M. Rice, S.X. Wang, R.L. White, S.H. Sun, Nano Lett. 5 (2005) 379.
[13] T. Härtling, T. Uhlig, A. Seidenstücker, N.C. Bigall, P. Olk, Appl. Phys. Lett. 96 (2010) 183111.
[14] H.W. Gu, R.K. Zheng, X.X. Zhang, B. Xu, J. Am. Chem. Soc. 126 (2004) 5664.
[15] S.O. Obare, R.E. Hollowell, C.J. Murphy, Langmuir 18 (2002) 10407.
[16] Y. Kim, R.C. Johnson, J.T. Hupp, Nano Lett. 1 (2001) 165.
[17] K. Aslan, J. Zhang, J.R. Lakowicz, C.D. Geddes, J. Fluoresc. 14 (2004) 391.
[18] J.N. Anker, W.P. Hall, O. Lyandres, N.C. Shah, J. Zhao, R.P. Van Duyne, Nat. Mater. 7 (2008) 442.
[19] N.S. Eum, S.H. Yeom, D.H. Kwon, H.R. Kim, S.W. Kang, Sens. Actuators B 143 (2010) 784.
[20] P.K. Jain, S. Eustis, M.A. El-Sayed, J. Phys. Chem. B 110 (2006) 18243.
[21] H. Zhang, D.Q. Song, S. Gao, H.Q. Zhang, J. Zhang, Y. Sun, Talanta 115 (2013) 857.
[22] S.G. Grancharov, H. Zeng, S. Sun, S.X. Wang, S. O'Brien, C.B. Murray, J.R. Kirtley, G.A. Held, J. Phys. Chem. B 109 (2005) 13030.
[23] S.H. Hu, C.H. Tsai, C.F. Liao, D.M. Liu, S.Y. Chen, Langmuir 24 (2008) 11811.
[24] A. Ito, M. Shinkai, H. Honda, T. Kobayashi, J. Biosci. Bioeng. 100 (2005) 1.
[25] Y.M. Huh, Y.W. Jun, H.T. Song, S.J. Kim, J.S. Choi, J.H. Lee, S. Yoon, K.S. Kim, J. S. Shin, J.S. Suh, J. Cheon, J. Am. Chem. Soc. 127 (2005) 12387.
[26] L.Y. Wang, Y. Sun, J. Wang, X.N. Zhu, F. Jia, Y.B. Cao, X.H. Wang, H.Q. Zhang, D. Q. Song, Talanta 78 (2009) 265.
[27] B.K. Oh, Y.K. Kim, W. Lee, Y.M. Bae, W.H. Lee, J.W. Choi, Biosens. Bioelectron. 18 (2003) 605.
[28] R. Karlsson, J. Mol. Recognit. 17 (2004) 15.

[29] X. Liu, Y. Sun, D.Q. Song, Q.L. Zhang, Y. Tian, H.Q. Zhang, Talanta 68 (2006) 1026.
[30] M.G. Manera, G. Leo, M.L. Curri, P.D. Cozzoli, R. Rella, P. Siciliano, A. Agostiano, L. Vasanelli, Sens. Actuators B 100 (2004) 75.
[31] J. Wang, D.Q. Song, L.Y. Wang, H. Zhang, H.Q. Zhang, Y. Sun, Sens. Actuators B 157 (2011) 547.
[32] H. Zhang, Y. Sun, S. Gao, J. Zhang, H.Q. Zhang, D.Q. Song, Small 9 (2013) 2537.
[33] Z.Y. Lu, G. Wang, J.Q. Zhuang, W.S. Yang, Colloids Surf. A 278 (2006) 140.
[34] B. Nikoobakht, M.A. El-Sayed, Chem. Mater. 15 (2003) 1957.
[35] Y. Negishi, K. Nobusada, Y. Tsukuda, J. Am. Chem. Soc. 127 (2005) 5261.
[36] J.J. Suñol, M.E. Bonneau, L. Roué, D. Guay, R. Schulz, Appl. Surf. Sci. 158 (2000) 252.
[37] J. Homola, I. Koudela, S.S. Yee, Sens. Actuators B 54 (1999) 16.